

1 **Supplementary Information for**

2
3 **High-throughput drug target discovery by fully automated proteomics**
4 **sample preparation platform**
5

6 **Qiong Wu^{a,†}, Jiangnan Zheng^{a,†}, Xintong Sui^{a,†}, Changying Fu^{a,†}, Xiaozhen Cui^a, Bin Liao^a, Hongchao**
7 **Ji^a, Yang Luo^a, An He^a, Xue Lu^a, Xinyue Xue^a, Chris Soon Heng Tan^{a,b,*}, Ruijun Tian^{a,b,*}**

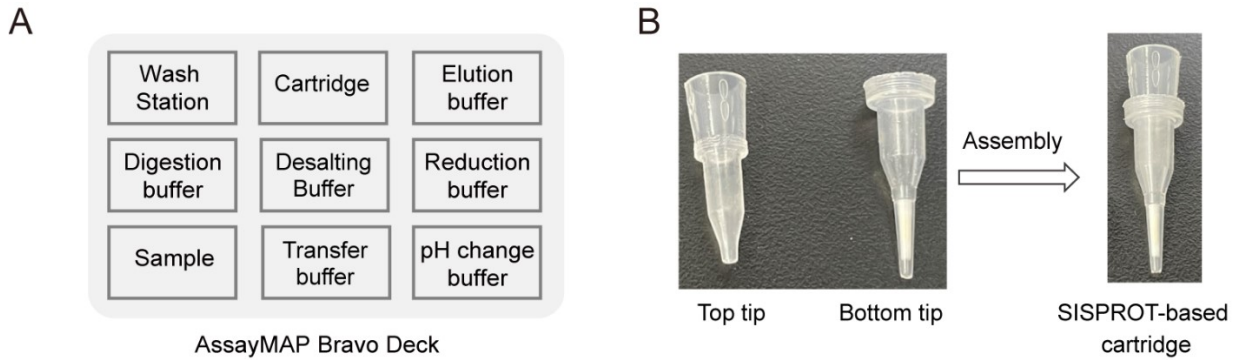
8
9 ^a Department of Chemistry, School of Science, Southern University of Science and Technology, Shenzhen
10 518055, China;

11 ^b Research Center for Chemical Biology and Omics Analysis, School of Science, Southern University of
12 Science and Technology, 1088 Xueyuan Road, Shenzhen 518055, China;

13 [†] These authors contributed equally to this manuscript.

14 *Correspondence authors: Ruijun Tian (tianrj@sustech.edu.cn); Chris Soon Heng Tan
15 (chris.tan.sh@gmail.com).

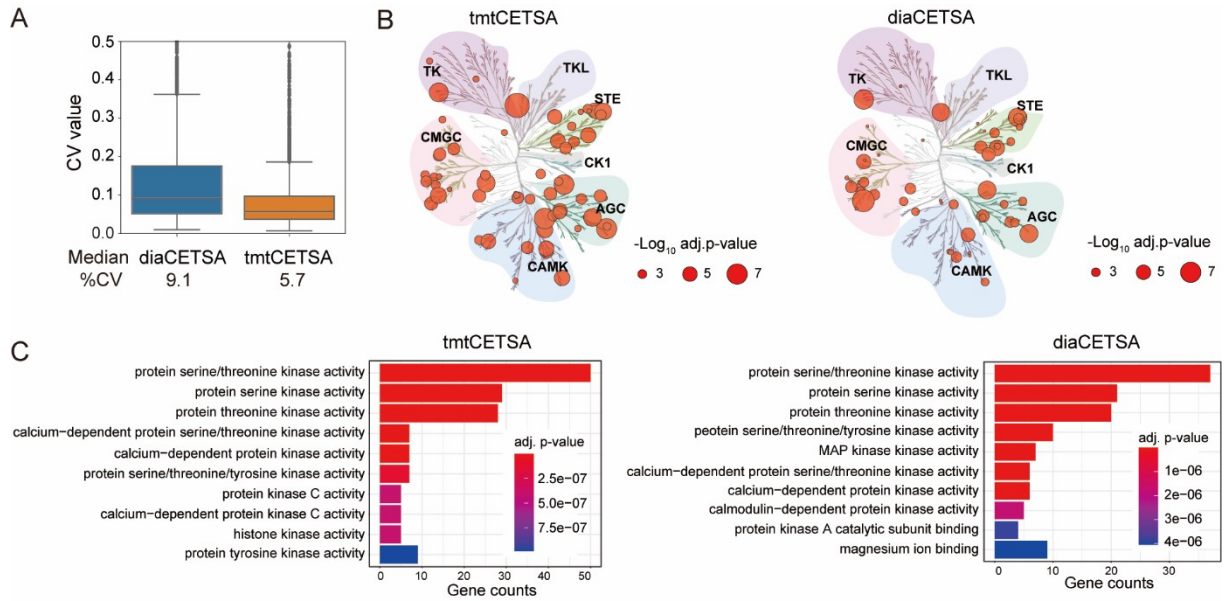
22



23

24 **Fig. S1 The setup of autoSISPROT.** (A) The setup of the AssayMAP Bravo deck. (B) The SISPROT-based
25 cartridges are created by assembling top and bottom tips that contain C18 membrane and mixed SCX/SAX
26 beads. The preparation of SISPROT-based cartridges followed a strict ten-step process, and a three-step
27 operating procedure was used as a rigorous quality control to ensure the reproducibility of the SISPROT-based
28 cartridges.

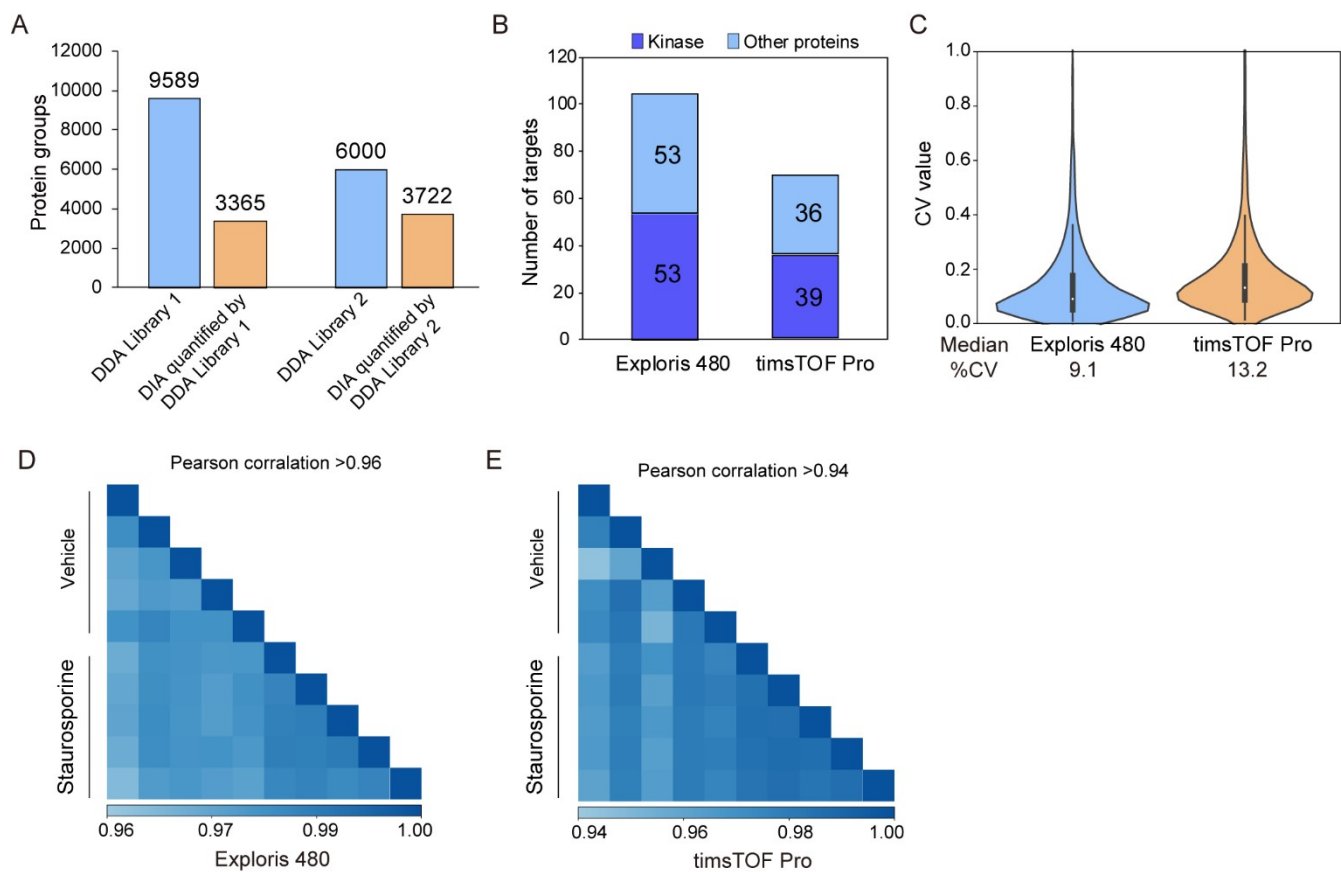
29



31

32 **Fig. S2 Comparison of the tmtCETSA and diaCETSA.** (A) Violin plots showing the distributions of CVs
 33 of protein intensities between tmtCETSA and diaCETSA ($n = 5$ technical replicates). (B) Kinome tree
 34 displaying all staurosporine kinase targets identified by using tmtCETSA and diaCETSA. Circle size is
 35 proportional to the $-\log_{10}$ adjust p-value. (C) GO annotation of molecular function for all the identified
 36 significant proteins by using tmtCETSA and diaCETSA.

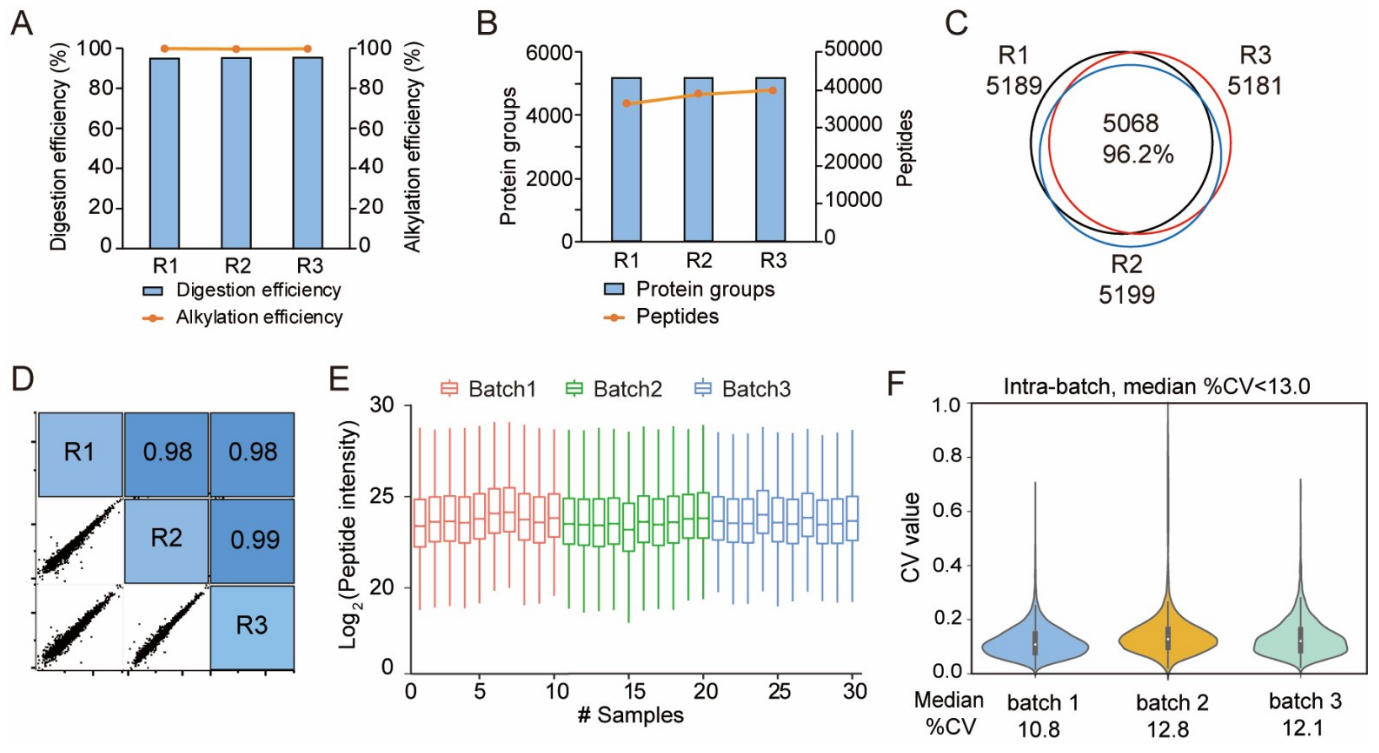
37



38

39 **Fig. S3 The optimization of diaCETSA.** (A) Bar charts showing DIA quantified protein groups by searching
 40 with different project-specific libraries. (B) The number of significant staurosporine targets analyzed using
 41 Exploris 480 and timsTOF Pro. (C) Violin plots depicting CVs of protein intensities for the analysis of
 42 diaCETSA samples. (D, E) Pearson correlation coefficient of protein intensities for the diaCETSA samples in
 43 the (D) Exploris 480 and (E) timsTOF Pro experiments.

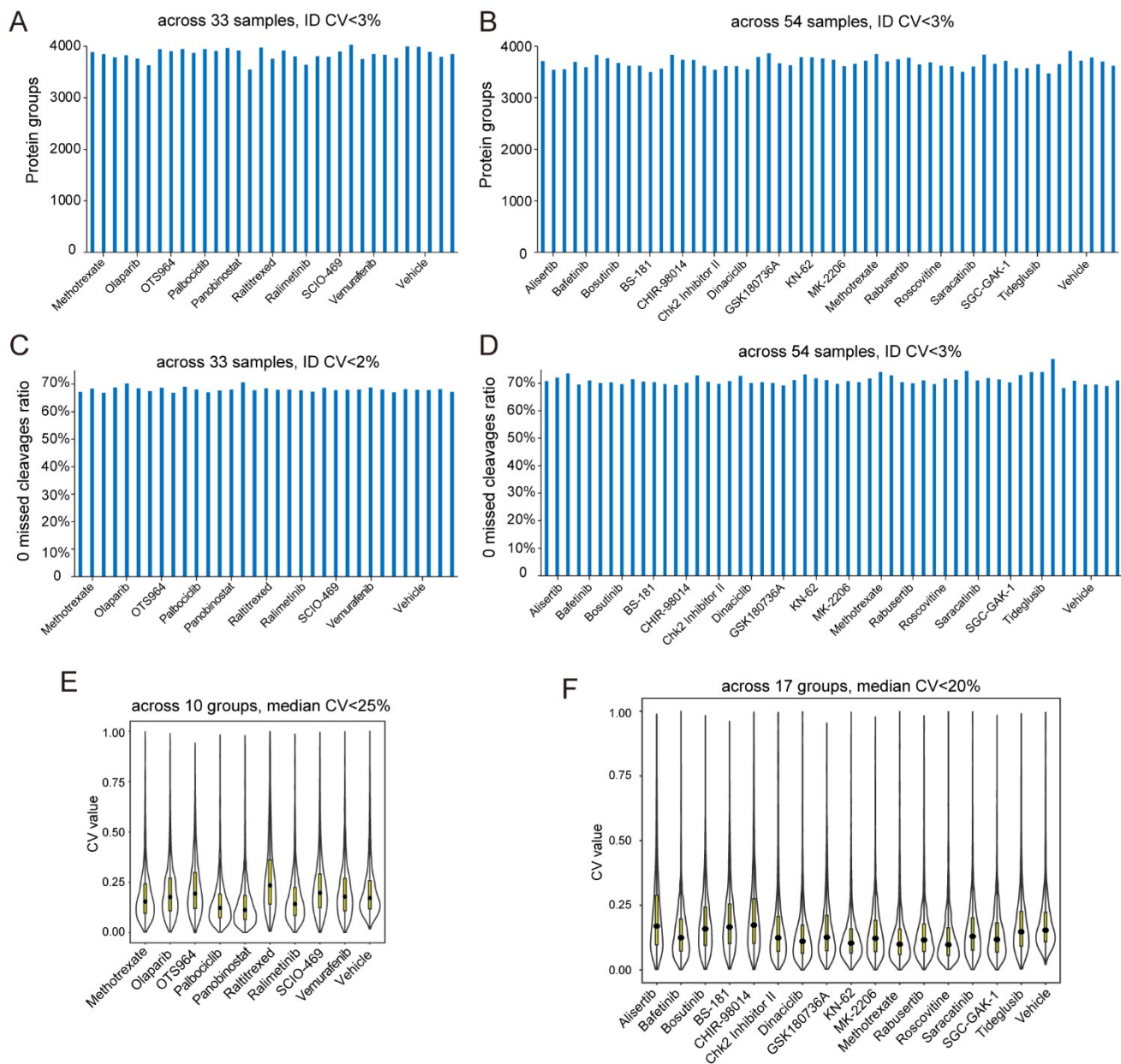
44



45

46 **Fig. S4 Performance of the proteome profiling by using autoSISPROT.** (A) Alkylation and digestion
 47 efficiencies of autoSISPROT for processing 10 μ g of HEK 293T cell lysates under three technical replicates.
 48 (B) The number of protein groups and peptides identified with DIA. (C) The number of common protein
 49 groups identified by autoSISPROT identified with DIA under three technical replicates. (D) Correlation of
 50 LFQ intensities of proteins quantified with DIA under three technical replicates. (E) Boxplots of log₂-
 51 transformed peptide intensities across three batches samples. The color coding highlights the samples batch
 52 of origin. (F) Violin plots depicting CVs distribution of protein LFQ intensities within the same batch. CV
 53 values are calculated with a minimum of three valid values within each batch.

54



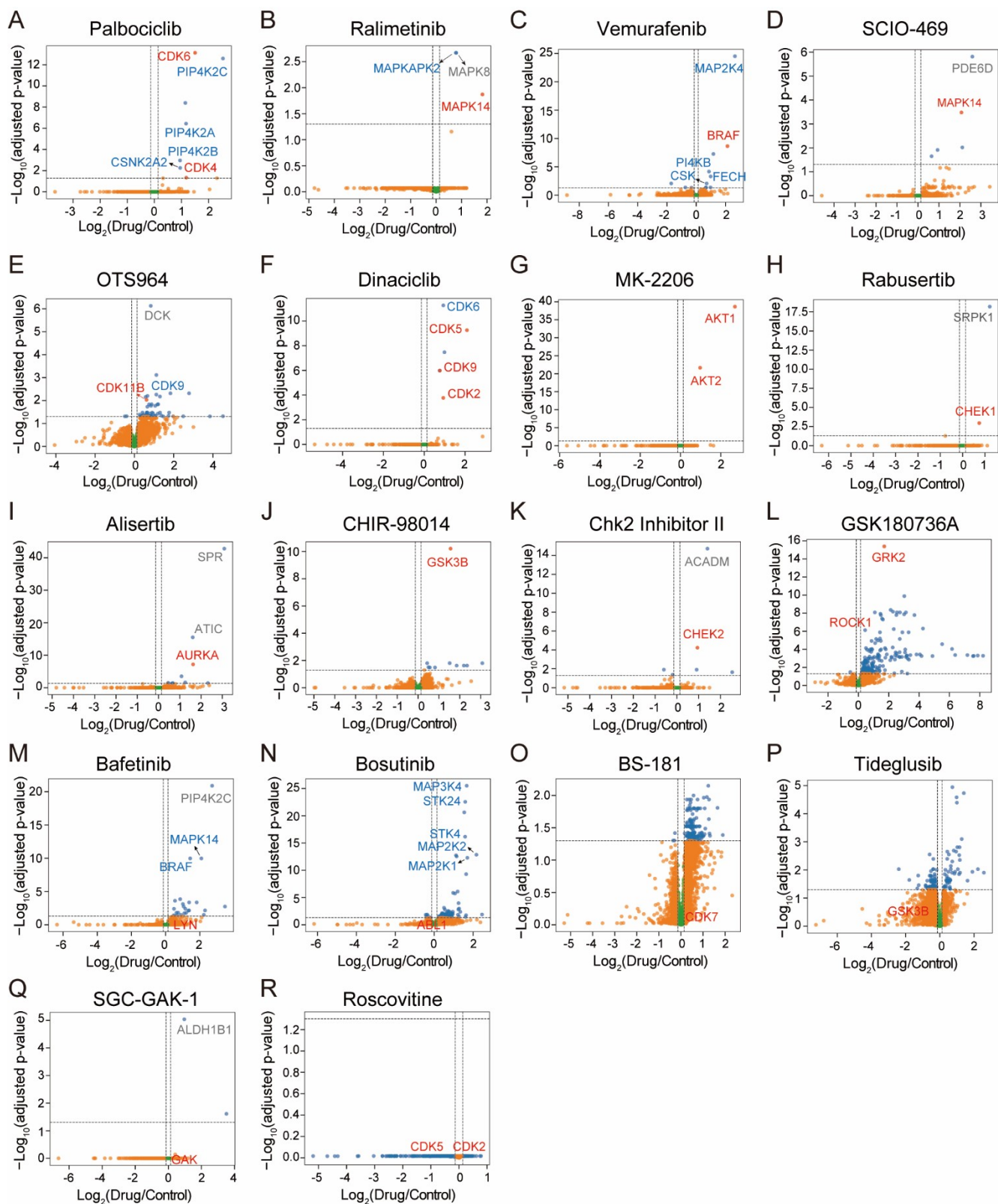
55

56 **Fig. S5 Sample preparation performance of autoSISPROT for high-throughput drug target**
 57 **identification.** (A, B) The number of protein groups identified in (A) batch 1 (33 samples) and (B) batch 2
 58 (54 samples). (C, D) The percentages of zero missed cleavages in (C) batch 1 and (D) batch 2. (E, F) Violin
 59 plots depicting CVs distribution of protein LFQ intensities from (E) batch 1 and (F) batch 2.

60

61

62



63

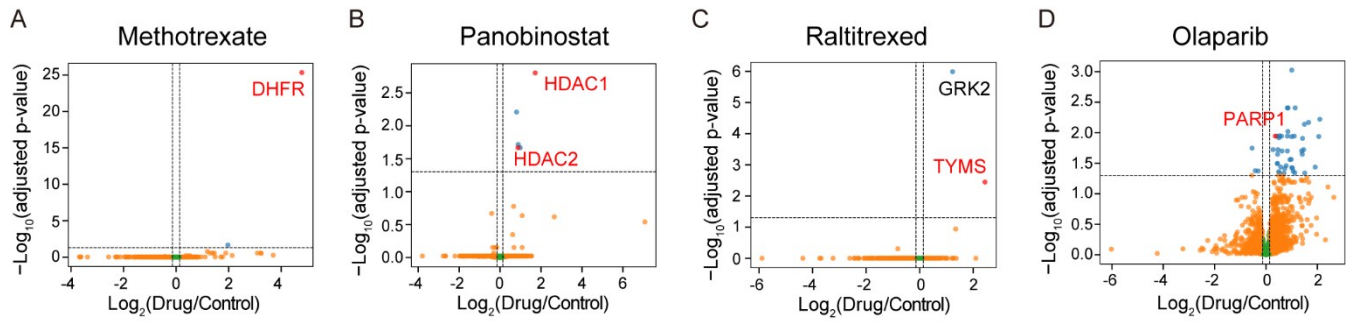
64 **Fig. S6** Volcano plots showing the identified drug targets from K562 cell lysates. (A) palbociclib; (B)
 65 ralimetinib; (C) vemurafenib; (D) SCIO-469; (E) OTS964; (F) dinaciclib; (G) MK-2206; (H) rabusertib; (I)
 66 alisertib; (J) CHIR-98014; (K) Chk2 inhibitor II; (L) GSK180736A; (M) bafetinib; (N) bosutinib; (O) BS-
 67 181; (P) tideglusib; (Q) SGC-GAK-1; (R) roscovitine. The negative controls, referred to as the “pooled
 68 control”¹, consisted of a combination of the vehicle and all other drug treatment conditions. However, drugs

69 sharing the same target were not included in the pooled controls for a specific drug. For instance, the SCIO469
70 and ralimentib treatment groups were not included in the pooled control for each other. Similarly, the bosutinib
71 treatment group was excluded from the pooled control for the Chk2 Inhibitor II target identification. Adjusted
72 p-value=0.05 is indicated by a solid horizontal line. The known targets are marked in red circle and the other
73 significant proteins are marked in blue circle. The known targets are highlighted in red, while the reported off-
74 targets were highlighted in blue.

75

76

77



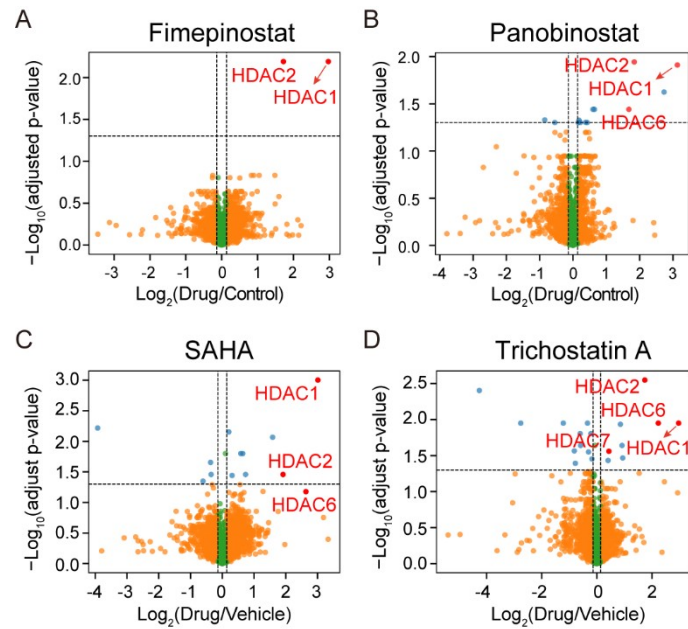
79

80 **Fig. S7 Volcano plots showing the identified drug targets from K562 cell lysates, performed at 52 °C.**

81 (A) methotrexate; (B) panobinostat; (C) raltitrexed; (D) olaparib. The pooled control consisted of a
 82 combination of the vehicle and all other drug treatment conditions, which were used as the negative controls.
 83 Adjusted p-value=0.05 is indicated by a solid horizontal line. The known targets are marked in red circle and
 84 the other significant proteins are marked in blue circle. The known targets are highlighted in red.

85

86



87

88 **Fig. S8** Volcano plots showing the identified drug targets from K562 cell lysates, performed at 52 °C.

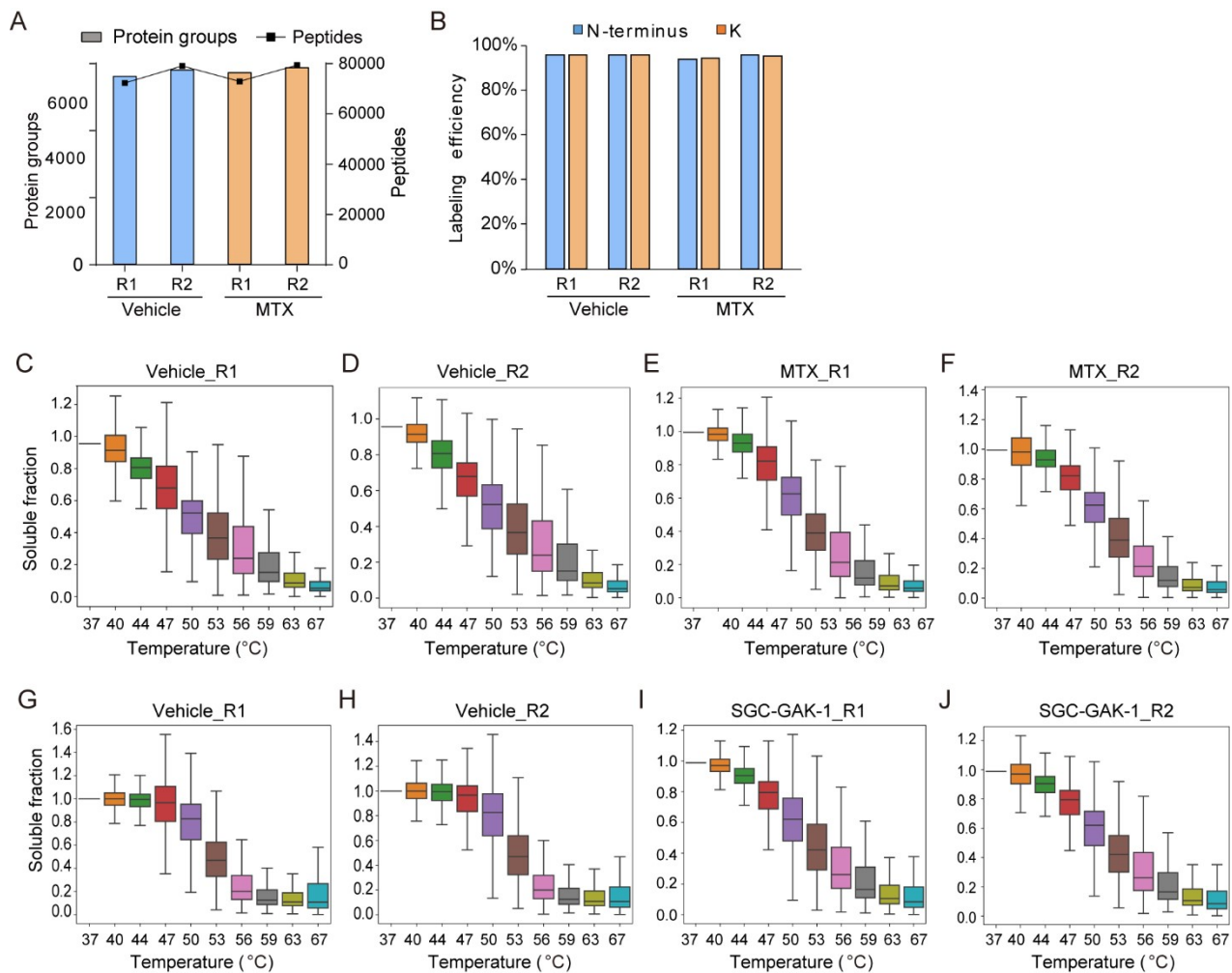
89 (A) fimepinostat; (B) panobinostat; (C) SAHA; (D) olaparib. The DMSO vehicle was used as the negative

90 control. Adjusted p-value=0.05 is indicated by a solid horizontal line. The known targets are marked in red

91 circle and the other significant proteins are marked in blue circle. The known targets are highlighted in red.

92

93



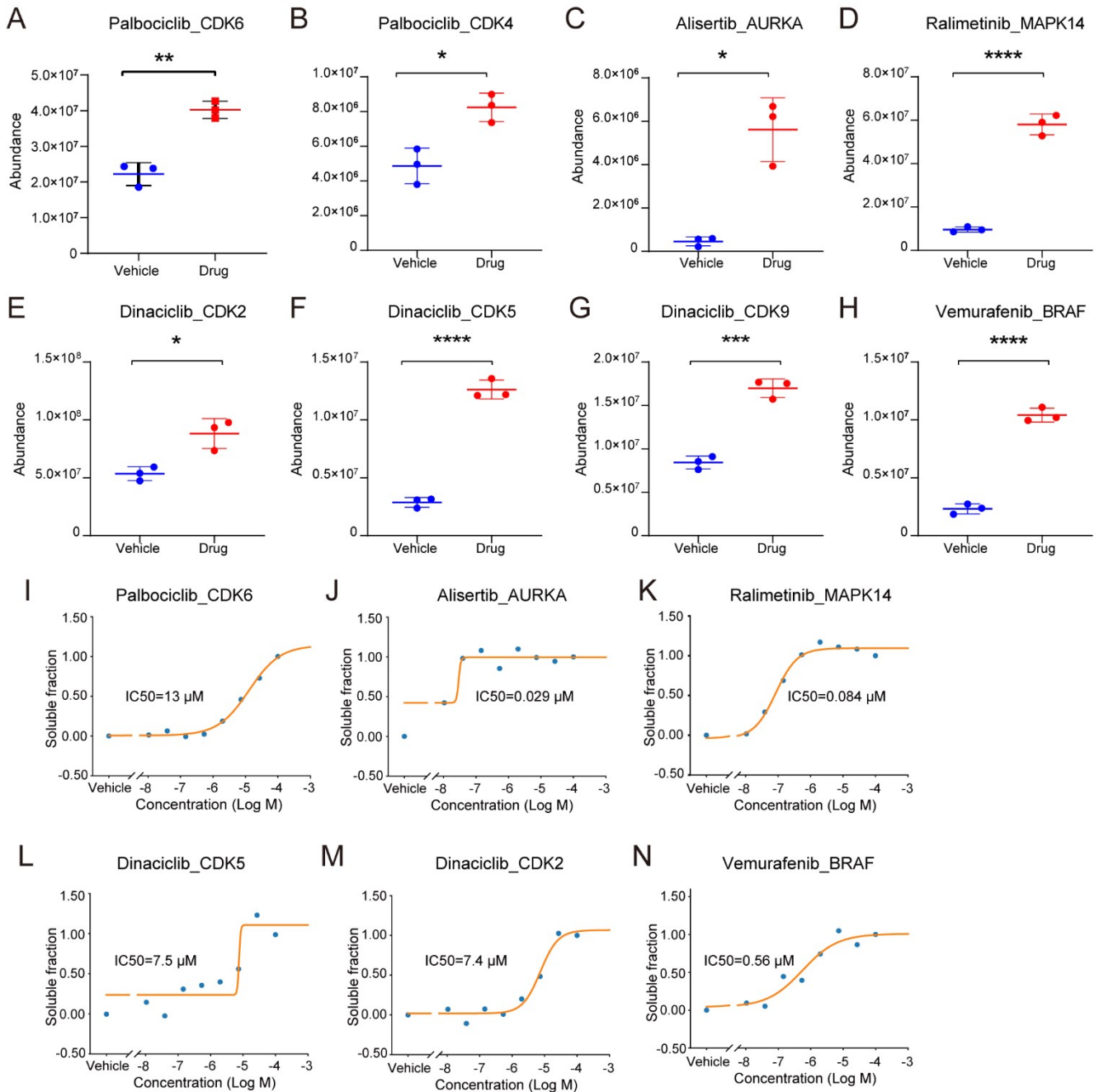
94

95 **Fig. S9 The identification of drug target of MTX by using CETSA and autoSISPROT.** (A) Protein and
 96 peptide identifications from two independent replicates per condition. (B) TMT labeling efficiency of peptide
 97 N-terminus and lysine residues for CETSA samples. (C-F) Boxplot of soluble fraction from indicated
 98 temperatures for (C) Vehicle_R1, (D) Vehicle_R2, (E) MTX_R1, and (F) MTX_R2, respectively. (G-J) Box
 99 plots of soluble fraction from indicated temperatures for (G) Vehicle_R1, (H) Vehicle_R2, (I) SGC-GAK-
 100 1_R1, and (J) SGC-GAK-1_R2, respectively.

101

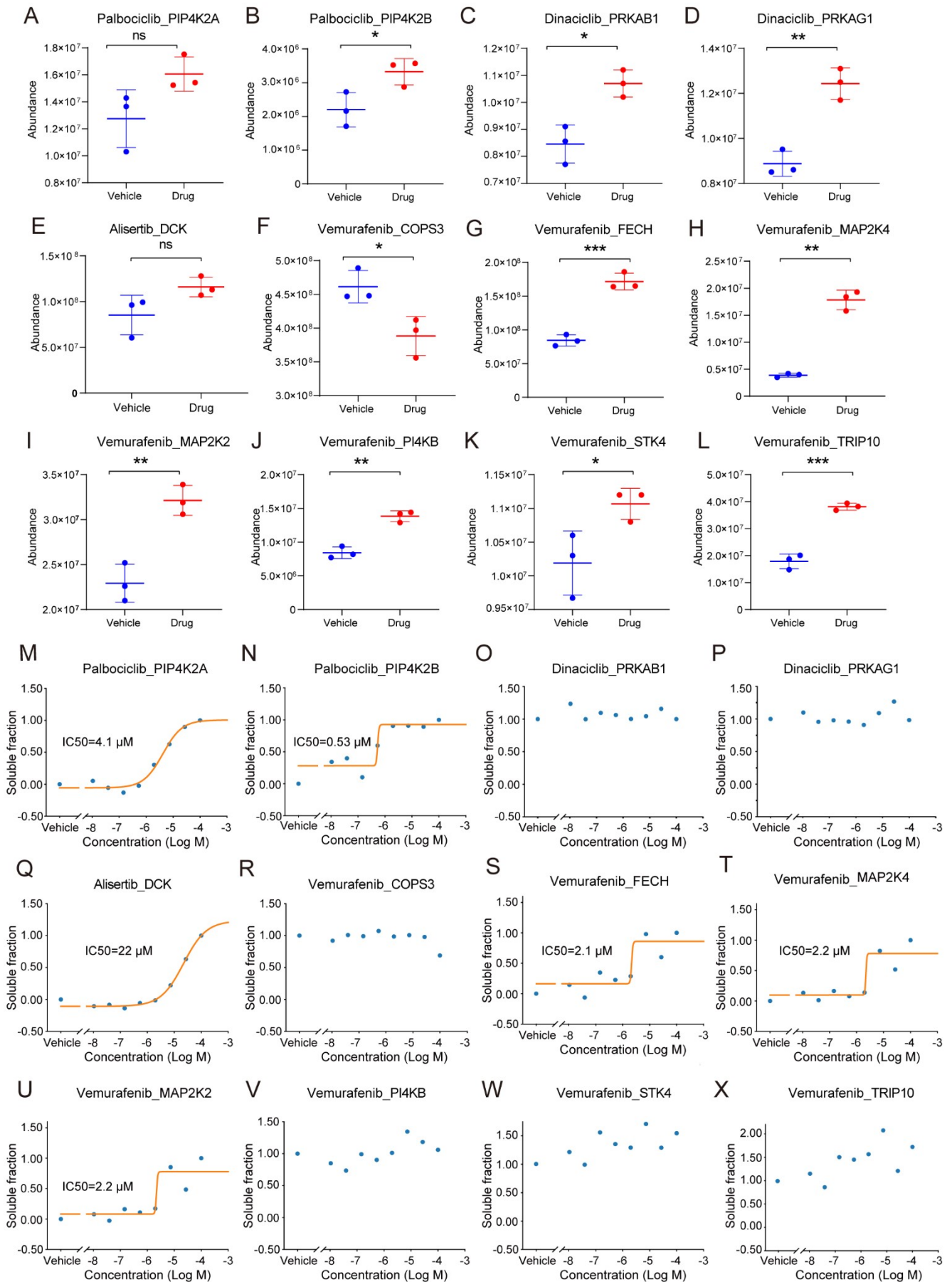
102

103



104

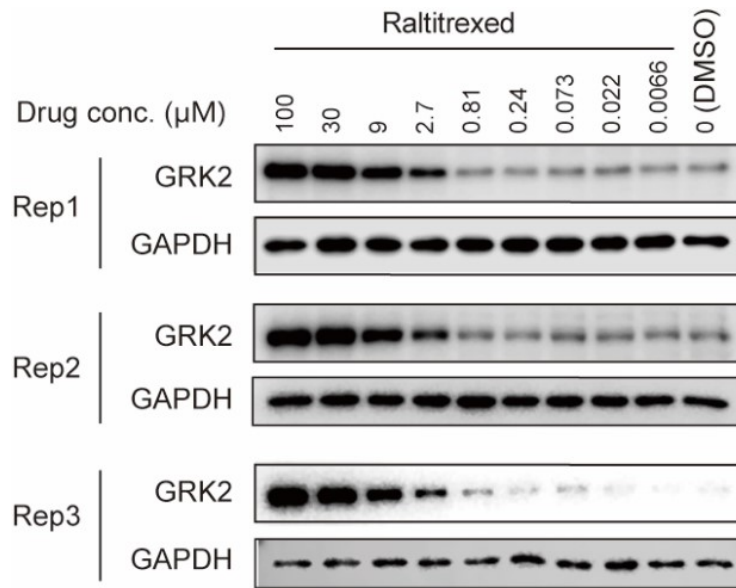
105 **Fig. S10 Target validation by PRM assay.** (A-H) K562 cell lysates were treated with 20 μM drug or vehicle,
 106 followed by thermal treatment at 52 °C. Selected targets for PRM assay were (A) CDK6, (B) CDK4, (C)
 107 AURKA, (D) MAPK14, (E) CDK2, (F) CDK5, (G) CDK9, and (H) BRAF. (I-N) ITDR experiments at 52 °C
 108 with treatment of eight concentrations (100, 27, 7.3, 2.0, 0.53, 0.14, 0.039, and 0.010 μM) of drug and vehicle,
 109 followed by thermal treatment at 52 °C. (I) CDK6, (J) AURKA, (K) MAPK14, (L) CDK5, (M) CDK2, (N)
 110 BRAF.



111

112 **Fig. S11 Off-target validation by PRM assay.** (A-L) K562 cell lysates were treated with 20 μM drug or

113 vehicle, followed by thermal treatment at 52 °C. Selected targets for PRM assay were (A) PIP4K2A, (B)
114 PIP4K2B, (C) PRKAB1, (D) PRKAG1, (E) DCK, (F) COPS3, (G) FECH, (H) MAP2K4, (I) MAP2K2, (J)
115 PI4KB, (K) STK4, and (L) TRIP10. (M-X) ITDR experiments at 52 °C with treatment of eight concentrations
116 (100, 27, 7.3, 2.0, 0.53, 0.14, 0.039, and 0.010 µM) of drug and vehicle, followed by thermal treatment at 52
117 °C. (M) PIP4K2A, (N) PIP4K2B, (O) PRKAB1, (P) PRKAG1, (Q) DCK, (R) COPS3, (S) FECH, (T)
118 MAP2K4, (U) MAP2K2, (V) PI4KB, (W) STK4, and (X) TRIP10.



120

121 **Fig. S12 Western blot-based ITDR CETSA for GRK2 at 52°C.** K562 cell lysates were treated with
 122 different concentration of drug in DMSO or with DMSO alone, and heated at 52 °C for 3 min. The protein
 123 aggregates were removed by centrifugation, and the soluble fractions were subjected to western blot analysis.

124

125

126

127

129 **Reference**

130

- 131 1. A. Lundby, G. Franciosa, K. B. Emdal, J. C. Refsgaard, S. P. Gnosa, D. B. Bekker-Jensen, A. Secher, S. R. Maurya, I. Paul,
132 B. L. Mendez, C. D. Kelstrup, C. Francavilla, M. Kveiborg, G. Montoya, L. J. Jensen and J. V. Olsen, Oncogenic Mutations
133 Rewire Signaling Pathways by Switching Protein Recruitment to Phosphotyrosine Sites, *Cell*, 2019, **179**, 543-560.e526.

134